3D Geometry and Quantitative Variation of the Cervico-Thoracic Region in Crocodylia

BEATRIZ CHAMERO,[1,2] ÁNGELA D. BUSCALIONI,[2]* JESÚS MARUGÁN-LOBÓN,[2,3] AND IOANNIS SARRIS[2]

[1]Museo Paleontológico Egidio Feruglio, Depto. Paleontología de Vertebrados, Av. Fontana 140, Trelew, Patagonia, Argentina

[2]Unidad de Paleontología. Dpto. de Biología, Universidad Autónoma de Madrid, Spain

[3]Dinosaur Institute, Natural History Museum of Los Angeles County, Los Angeles, California, USA

ABSTRACT

This study aims to interpret the axial patterning of the crocodylian neck, and to find a potential taxonomic signal that corresponds to vertebral position. Morphological variation in the cervico-thoracic vertebrae is compared in fifteen different crocodylian species using 3D geometric morphometric methods. Multivariate analysis indicated that the pattern of intracolumnar variation was a gradual change in shape of the vertebral series (at the parapophyses, diapophyses, prezygapohyses, and postzygapohyses), in the cervical (C3 to C9) and dorsal (D1-D2) regions which was quite conservative among the crocodylians studied. In spite of this, we also found that intracolumnar shape variation allowed differentiation between two sub regions of the crocodylian neck. Growth is subtly correlated with vertebral shape variation, predicting changes in both the vertebral centrum and the neural spine. Interestingly, the allometric scaling for the pooled sample is equivalently shared by each vertebra studied. However, there were significant taxonomic differences, both in the average shape of the entire neck configuration (regional variation) and by shape variation at each vertebral position (positional variation) among the necks. The average neck vertebra of crocodylids is characterized by a relatively cranio-caudally short neural arch, whereby the spine is relatively longer and pointed orthogonal to the frontal plane. Conversely, the average vertebra in alligatorids has cranio-caudally longer neural spine and arch, with a relatively (dorso-ventrally) shorter spine. At each vertebral position there are significant differences between alligatorids and crocodylids. We discuss that the delayed timing of neurocentral fusion in Alligatoridae possibly explains the observed taxonomic differences. Anat Rec, 00:000–000, 2014. © 2014 Wiley Periodicals, Inc.

Key words: alligatoridae; crocodylidae; geometric morphometrics; interspecific allometry; neck organization

Eusuchian crocodiles are characterized by key skeletal evolutionary innovations including procoelous vertebrae, convex caudal articular surface, along their vertebral column, and a tetraseriated osteodermal shield (Norell, 1989; Busbey, 1994; Brochu 1997; Salisbury et al., 2006; Pol et al., 2009; Buscalioni et al., 2011). Early seminal contributions on vertebral shape posited that the acquisition of a procoelic vertebral articulation was the key skeletal modification that led to the emergence of the

Grant sponsor: MICIN (Spain); Grant number: AP2005-0677; Grant sponsor: Spanish Government; Grant number: CGL2009–11838; Grant sponsor: Argentinian CONICET.

*Correspondence to: Ángela D. Buscalioni, Unidad de Paleontología. Dpto de Biología. Universidad Autónoma de Madrid. C/Darwin 2, 28049 Cantoblanco, Madrid, Spain.
E-mail: angela.delgado@uam.es

Received 16 December 2013; Accepted 4 March 2014.

DOI 10.1002/ar.22926

Published online 00 Month 2014 in Wiley Online Library (wileyonlinelibrary.com).

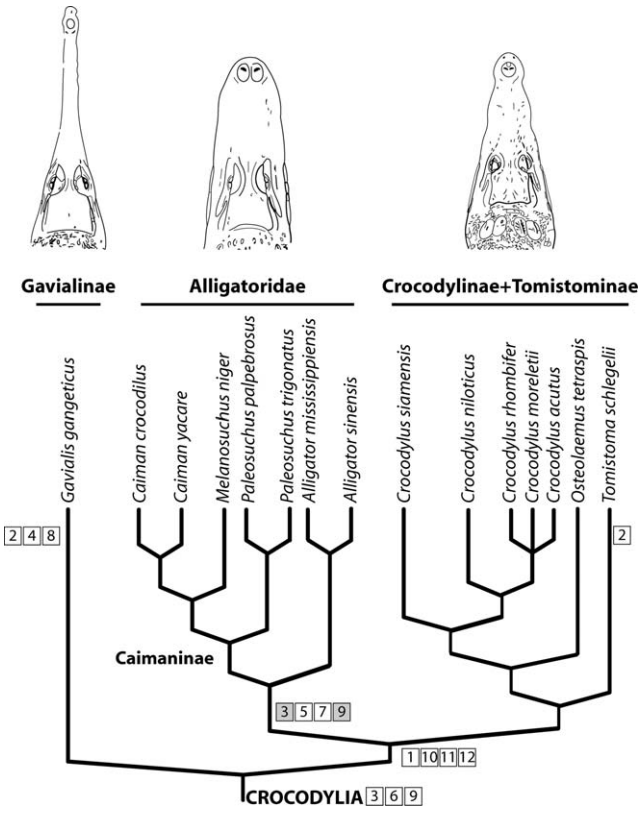

Fig. 1. Cladogram depicting the relationships between the species sampled, in which the main transformations of cervical characters are highlighted. The phylogenetic hypothesis and the definition of the derived character states are based on Brochu (1997): 1, Ventral tubercle of the proatlas less than one half; 2, Proatlas strap-shaped (1), massive and block shaped (2); 3, Caudal half of axis neural spine narrow; 4, Axis neural arch possesses a lateral process; 5, Atlas intercentrum plate-shaped in lateral view; 6, Axial hypapophysis located toward the cranial end of the vertebral body; 7, Hypapophyseal keels present on all cervical vertebrae, along thoracic vertebrae I–III (1), or thoracic vertebrae I–IV (2); 8, C-III with a weakly developed hypapophysis (1); or with a prominent hypapophysis (2); 9, Neural spines on the caudal cervical vertebrae craniocaudally narrow compared with those on the cranial cervical vertebrae; 10, Proatlas lacking a cranial process; 11: Cranial half of axis neural slopes cranially; 12, Axial neural spine not crested. Character state changes are placed according to an accelerate transformation optimization; the grey box are reversals.

clade Crocodylia (*sensu* Benton and Clark, 1988). This type of "ball and socket" vertebral articulation enabled enhanced angular movement with each vertebral unit, thereby increasing axial mobility in these animals. The mechanical advantages of the procoelic vertebrae, the presence of a biconvex first caudal vertebra and the angled disposition of the zygapophyses, signified an efficient progression towards aquatic life in crocodiles (Troxell, 1925). Several authors have suggested that the coupling of such key innovations (i.e., procoelia and dermal skeleton), would be biomechanically constraining both the musculoskeletal and dermatoskeletal systems (i.e., the Eusuchian bracing system *sensu* Salisbury and Frey, 2001; Salisbury et al., 2006), which restrained decisive phenotypic changes among major crocodylian clades (Cleuren and de Vree, 2000). In fact, Crocodylidae, Alligatoridae and the long-snouted genus *Gavialis* maintained the same musculoskeletal axial morphology (Seidel, 1978; Cleuren and De Vree, 2000; Tsuihiji, 2005, 2007).

As a consequence of the above, most of the morphological characters proposed for phylogenetic inference focus on the anatomy of the atlas-axis complex, the anatomy of the third cervical vertebra, and the extension of the hypapophyses to the dorsal vertebral series (see character description in Fig. 1). This leaves an important gap in our understanding of other taxonomic traits of the axial skeleton, in particular those relating to the cervicothoracic region, which may allow differentiating between major crocodilian clades. The fact that the cervical system is influenced by multiple factors and forces that stem from head support and limb movement (Frey, 1988a; Cleuren and de Vree, 2000), indicate the relevance of the entire anatomical and functional system in crocodile evolution. Therefore it is important to carry out new research on this system in the Crocodylia crown-group divergence.

Vertebral shape variation has been studied quantitatively in anthropological and medical studies (Manfreda et al., 2006), and in several mammalian groups (Filler, 1986; Chen et al., 2005; Galliari et al., 2009). However, similar studies are rather scarce in other vertebrate groups, for example amphibians (Wake, 1980) and reptiles (snakes, Polly and Head, 2004; Sarris et al., 2012; varanids, Burnell et al., 2012). In addition, postcranial axial shape variation is serially continuous and previous studies investigating interspecific morphometric variation in complete segments (cervical and/or dorsal series) have concluded that it is possible to make a detailed description of the general axial patterning of the group, as well as to identify specific traits that allow for regional axial differentiation. Therefore, predicting relevant correlated changes along vertebral portions as determined by axial position is morphometrically possible (Polly and Head, 2004), as well as by taxonomic and functional specializations (Wake, 1980; Burnell et al., 2012). Using three dimensional geometric morphometrics, here we aim to quantitatively describe vertebral shape variation for the first time in crocodylians. This will be achieved by analysing the vertebrae of the cervico-thoracic segment from fifteen different species. In particular, we aim to interpret the patterning of axial organization in the neck of Crocodylia (i.e., regional shape variation), and to ascertain whether there is a taxonomic signal (differentiation between families) corresponding to vertebral position (i.e., positional shape variation).

MATERIAL AND METHODS

Specimens

The sample spanned a wide range of crocodylian diversity (63% of all species) and disparity. It included eight genera, and 15 species of adult and subadult specimens (*Alligator mississippiensis* Daudin 1802, *A. sinensis* Fauvel 1879, *Caiman crocodilus* Linnaeus 1758, *C. yacare* Daudin 1802, *Melanosuchus niger* Spix 1825, *Paleosuchus palpebrosus* Cuvier 1807, *P. trigonatus* Schneider 1801, *Crocodylus acutus* Cuvier 1807, *C. moreletii* Duméril and Bibron 1851, *C. niloticus* Laurenti 1768, *C. rhombifer* Cuvier 1807, *C. siamensis* Schneider 1801, *Osteolaemus tetraspis* Cope 1861, *Tomistoma schlegelii* Müller 1838, *Gavialis gangeticus* Gmelin 1789)

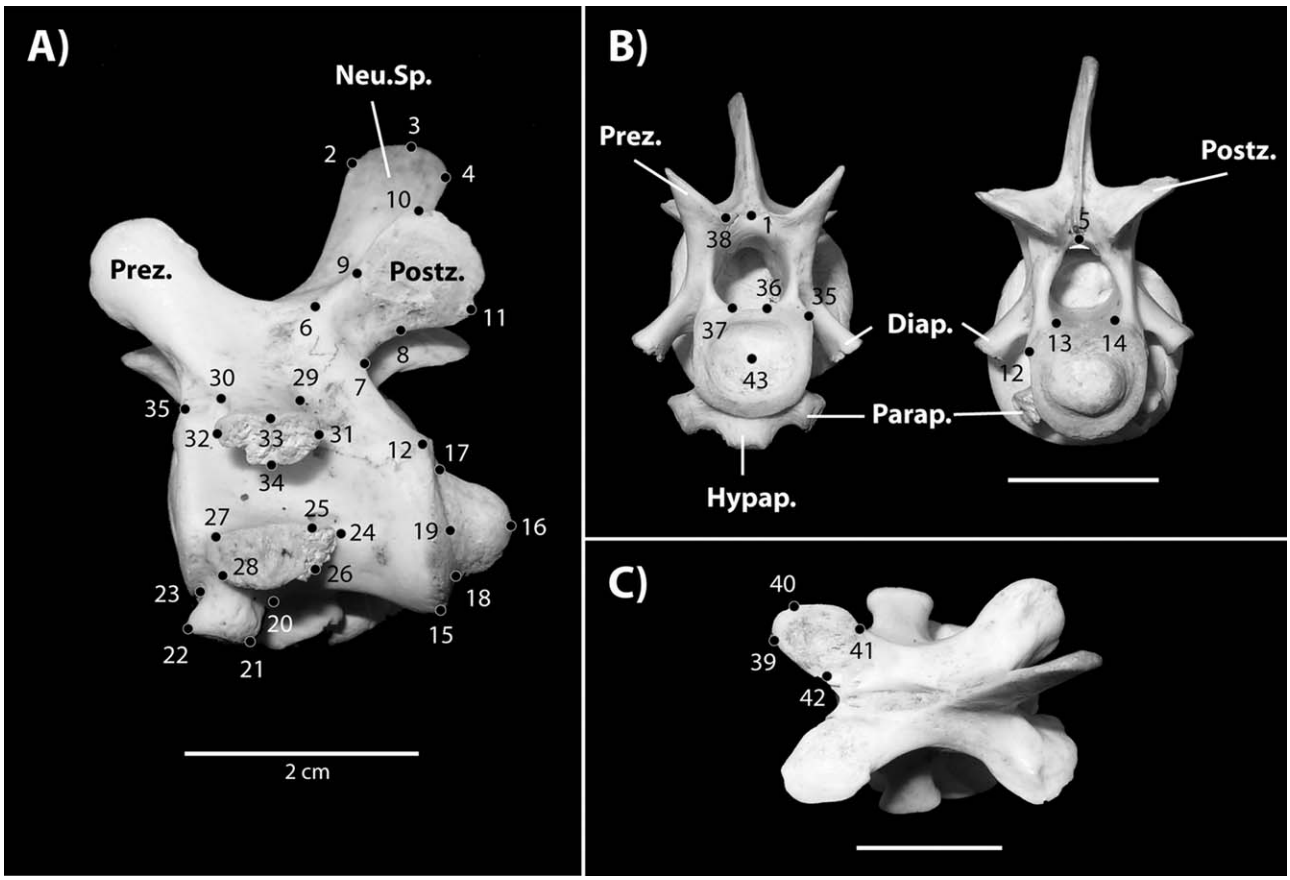

Fig. 2. Crocodylian cervical vertebra in lateral view (**A**), in cranial and caudal views (**B**) and in dorsal view (**C**) with the 43 landmarks described in Table 1. Scale bar 2 cm. Abbreviations: Diap., diapophysis; Hypap., hypapophysis; Neu.Sp., neural spine; Parap., parapophysis; Postz., postzygapophysis; Prez., prezygapophysis. CT-scanned vertebra from *Paleosuchus*.

all from the Florida Museum of Natural History (Gainesville, USA). The length of the femora was measured to determine the maturity of the specimens (see Appendix). In addition the occurrence of the neurocentral fusion in the specimens of *Alligator mississippiensis* was corroborated. According to Ikejiri's estimations (2012) the measurements that we obtained corresponded to those of adults, or nearly adult animals ranging between 1 and 3 m in body length.

The Cervico-thoracic Region

The ossification of the axial skeleton in crocodylians follows a cranio-caudal gradient. The cervical centra and neural arches show the first sign of mineralization during embryonic development (Rieppel, 1993). However, the fusion of the neural arch with the centrum occurs during postnatal ontogeny, leaving the neurocentral suture of most of the presacral vertebrae open, even after the animal reaches sexual maturity. Unlike the ossification pattern, the closure of the neurocentral suture follows a caudo-cranial sequence (Brochu, 1992). Therefore the neurocentral suture of the cervical region is the last to fuse. Consequently, the closure sequence of the external neurocentral suture can be traced along the axial series and compared with the body length of the animal (Ikejiri, 2012).

The presacral vertebral column in Crocodylia is divided into cervical and dorsal vertebrae that can be subdivided into thoracic and lumbar (Hoffstetter and Gasc, 1969). All the vertebrae are procoelous except for the atlas, the axis, the second sacral and the first caudal. Proof of the existence of at least seven cervical vertebrae is provided by the anterior extension of the coelom to the eighth vertebrae (Duncker, 1979), though osteological criteria restrict the cervical region to 8 or 9 vertebrae. Limiting the cervical region to the eighth cervical coincides with the position where the para- and diapophyses processes are furthest apart and situated near the dorsal central border (Mook, 1921). We define the cervical region as the nine first vertebrae restraining the series to those vertebrae bearing cervical ribs, which are disconnected from the sternum (Hoffstetter and Gasc, 1969; Frey, 1988b; Cleuren and De Vree, 2000; Claessens, 2009).

The classical approach to vertebral shape variation is essentially descriptive (Romer, 1956; Hoffstetter and Gasc, 1969), although occasionally some taxonomic studies involve the use of measurements (Mook, 1921, 1925; Johnson, 1955; Cong et al., 1998; Schwarz et al., 2006; Jouve et al., 2006). Overall, the vertebral series present a gradual morphological transition that depends on the position of the paired rib articulations (parapophysis with the costal capitulum, and diapophysis with the costal

TABLE 1. Vertebral landmarks anatomically ordered by: articular surfaces, bony processes, neural arch and centrum

No.	Anatomical description
	Articular Surfaces
15	Ventralmost border of the vertebral centrum on the caudal articular surface
16	Central distal tip of the vertebral condyle
17	Dorsalmost extreme of the vertebral condyle
18	Ventralmost extreme of the vertebral condyle
19	Lateralmost extreme of the vertebral condyle (left side)
25	Dorso-caudal border of the parapophysis capitular surface (pararthrum countour)
26	Ventro-caudal border of the parapophysis capitular surface (pararthrum countour)
27	Dorso-cranial border of the parapophysis capitular surface (pararthrum countour)
28	Ventro-cranial border of the parapophysis capitular surface (pararthrum countour)
31	Caudal border of the diapophysis tubercular surface (diarthrum countour)
32	Cranial border of the diapophysis tubercular surface (diarthrum countour)
33	Dorsal border of the diapophysis tubercular surface (diarthrum countour)
34	Ventral border of the diapophysis tubercular surface (diarthrum countour)
8	Cranio-axial border of the postzygapophysis articulation surface (postzygarthrum countour)
9	Cranio-lateral border of the postzygapophysis articulation surface (postzygarthrum countour)
10	Caudo-lateral border of the postzygapophysis articulation surface (postzygarthrum countour)
11	Caudo-axial border of the postzygapophysis articulation surface (postzygarthrum countour)
39	Cranio-axial border of the prezygapophysis articulation surface (prezygarthrum countour)
40	Cranio-lateral border of the prezygapophysis articulation surface (prezygarthrum countour)
41	Caudo-lateral border of the prezygapophysis articulation surface (prezygarthrum countour)
42	Caudo-axial border of the prezygapophysis articulation surface (prezygarthrum countour)
43	Central depression of the cranial cotyle (vertebral fossa)
	Vertebral Processes
24	Caudal contact between the parapophysis and the vertebral body (paraphophyseal process)
29	Caudal contact between the diapophysis and the vertebral body (diaphophyseal process)
30	Cranial contact between the diapophysis and the vertebral body (diaphophyseal process)
20	Caudal border of the hypapophysis at the vertebral body (hypaphophyseal process)
21	Ventro-caudal tip of the hypapophysis (hypaphophyseal process)
22	Ventro-cranial tip of the hypapophysis (hypaphophyseal process)
23	Cranial border of the hypapophysis at the vertebral centrum (hypaphophyseal process)
1	Axial confluence of the neural arch and the neural spine at the cranial region (spinal process)
2	Dorso-cranial contour of the neural spine (spinal process)
3	Neural spine maximum dorsal curvature (spinal process)
4	Dorso-caudal contour of the neural spine (spinal process)
5	Axial confluence of the neural arch and the neural spine at the caudal region (spinal process)
6	Cranio-lateral tip of the postzygapophysis pedicle (postzygapophyseal process)
7	Cranialmost tip of the postzygapophysis pedicle (postzygapophyseal process)
38	Cranial confluence between the neural arch and the right prezygapophysis (prezygapophyseal process)
	Neural arch and centrum
12	Lateral confluence of the left neural arch pedicle and the vertebral centrum on the neurocentral suture at the caudal region (peduncle of the neural arch)
13	Axial confluence of the left neural arch pedicle and the vertebral centrum on the neurocentral suture at the caudal region (peduncle of the neural arch)
14	Axial confluence of the right neural arch pedicle and the vertebral centrum on the neurocentral suture at the caudal region (peduncle of the neural arch)
35	Lateral confluence of the left neural arch pedicle and the vertebral centrum on the neurocentral suture at the cranial region (peduncle of the neural arch)
36	Axial confluence of the left neural arch pedicle and the vertebral centrum on the neurocentral suture) at the cranial region (peduncle of the neural arch)
37	Axial confluence of the right neural arch pedicle and the vertebral centrum (on the neurocentral suture) at the cranial region (peduncle of the neural arch)

The terminologies used follow Salisbury et al. (2006), and in bracket, Filler (1986).

tuberculum), and on the zygarthral (pre- and postzygapophyses) angles between adjacent vertebrae (Mook, 1921; Salisbury and Frey, 2001). Unlike those of Aves and some non-avian dinosaurs, the position and shape of parapophyses and diapophyses shifts continuously along the cervico (2–9) and thoracic (1–9) series in crocodylians (Mook, 1921; Claessens, 2009; Schachner et al., 2009). The area selected in this study comprises the third (C3) to the ninth (C9) cervical vertebrae, and the first two thoracic vertebrae (D1–2) where this gradual variation is clear. The atlas and axis have been excluded because each vertebra is formed by a singular combination of diverse and isolated elements whose configuration makes impossible any comparison with the rest of vertebrae. The first two thoracic vertebrae (prothoracic vertebrae, according Salisbury and Frey, 2001) have been included because they are more similar to the preceding cervical vertebrae than to the subsequent dorsal vertebrae.

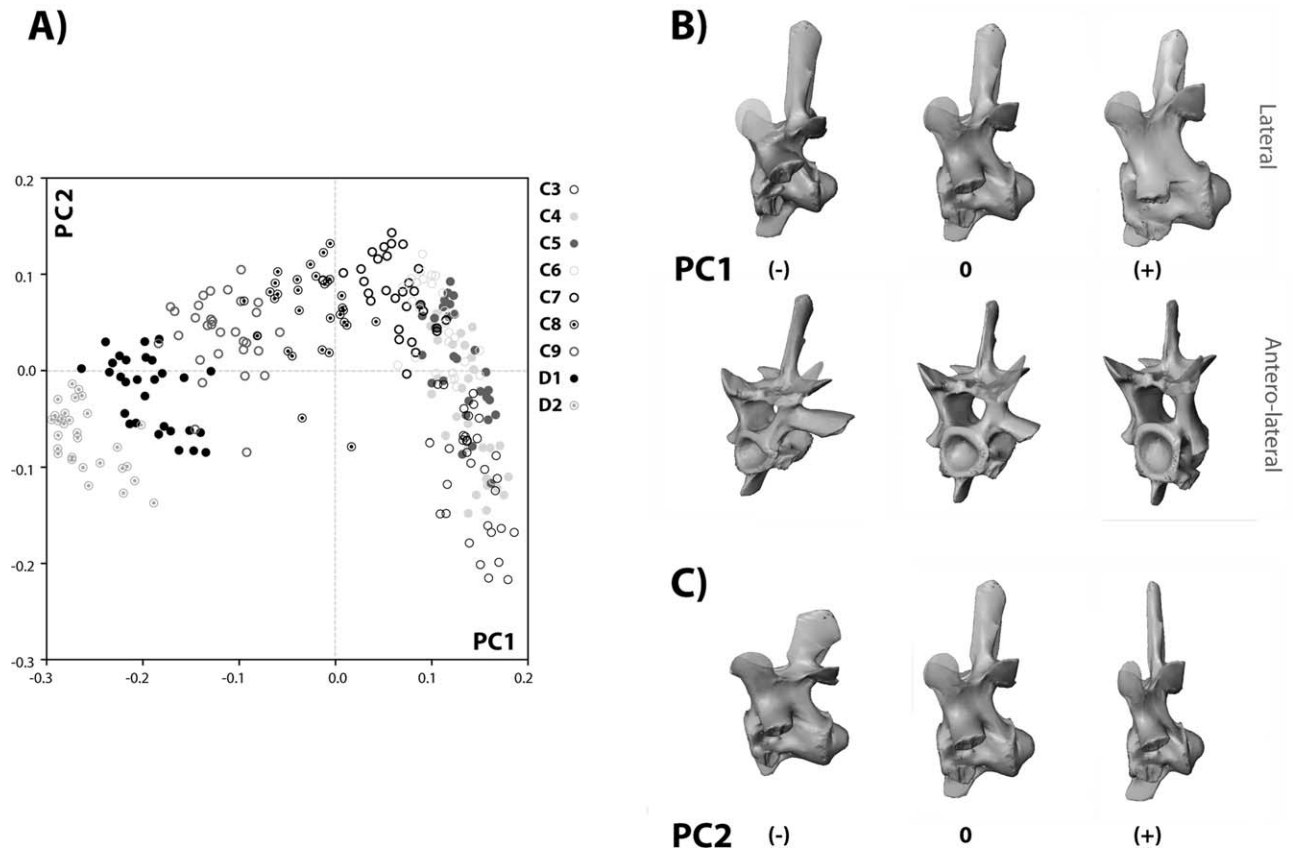

Fig. 3. Principal components of all the vertebrae (n = 277). (**A**) Scatter-plot of PC1 (*x* axis) versus PC2 (*y* axis). (**B**) Morphological variation across PC1. Vertebrae have been represented laterally and in their anterolateral views to show main variation at positive and negative values. (**C**) Morphological variation across PC2. Vertebrae represented in lateral view. Note that vertebrae in the anterolateral views are not fully symmetrical, because variation is captured solely at the left vertebral half and the right prezygapophysis (see Material and Methods). The left prezygaphophysis has been cleared to facilitate the view of the shape variation.

TABLE 2. PCA for regional variation (left) and positional variation (right)

	Regional variation				Positional variation			
PC	Eigenvalues	% Var	Cum %		PC	Eigenvalues	% Var	Cum %
1	0.02176757	51.16	51.16	**C3**	1	0.00605908	30.746	
2	0.00602996	14.172	65.333		2	0.00241363	12.248	42.994
3	0.00281452	6.615	71.948	**C4**	1	0.00609147	33.96	
4	0.00138955	3.266	75.213		2	0.00283418	15.8	49.76
5	0.00120852	2.84	78.054	**C5**	1	0.00481758	27.547	
6	0.00100114	2.353	80.407		2	0.00359374	20.549	48.096
7	0.00091019	2.139	82.546	**C6**	1	0.00469903	26.738	
8	0.00075779	1.781	84.327		2	0.00393106	22.368	49.106
9	0.00058606	1.377	85.704	**C7**	1	0.00494791	29.219	
10	0.0004912	1.154	86.859		2	0.00338565	19.994	49.213
11	0.00047194	1.109	87.968	**C8**	1	0.00417029	24.79	
12	0.00041704	0.98	88.948		2	0.00269363	16.012	40.803
13	0.00031541	0.741	89.69	**C9**	1	0.00392838	24.549	
14	0.00028307	0.665	90.355		2	0.00247795	15.485	40.034
				D1	1	0.00389559	23.073	
					2	0.00236315	13.996	37.069
				D2	1	0.00502134	28.669	
					2	0.00255951	14.613	43.282

For positional variation only the first two first principal components are indicated.

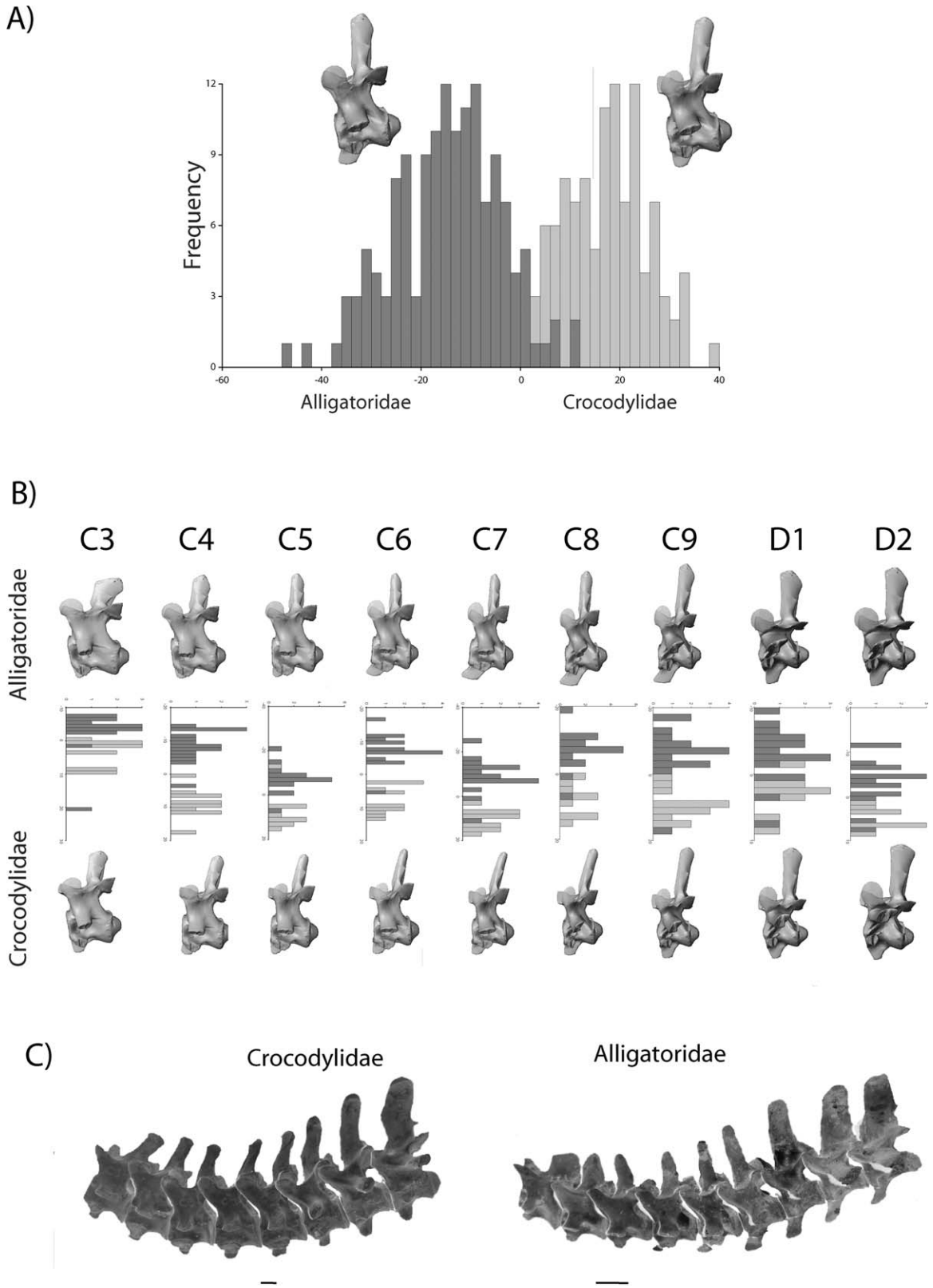

Fig. 4. Morphological differences between Alligatoridae and Crocodylidae. (**A**) Discrimant analysis showing the statistical difference in average vertebral shape ($P < 0.0001$) between families, considering the entire series (regional variation) (**B**) Discriminate analysis of mean shape differences by vertebral position between families (local variation). In (A) and (B) the images are thin-plate spline morphs representing the mean shape corresponding to each family. Notice that the likelihood of discriminating correctly decreases caudally. (**C**) Anatomical neck configuration in Crocodylidae (IHNE *Crocodylus acutus*, male, body length 300 cm), and Alligatoridae (IHNE *Caiman crocodilus*, male, body length 160 cm). Scale bar 2 cm. Specimens housed in Instituto de Historia Natural y Ecología, Museo del Cocodrilo, Estado de Chiapas, México.

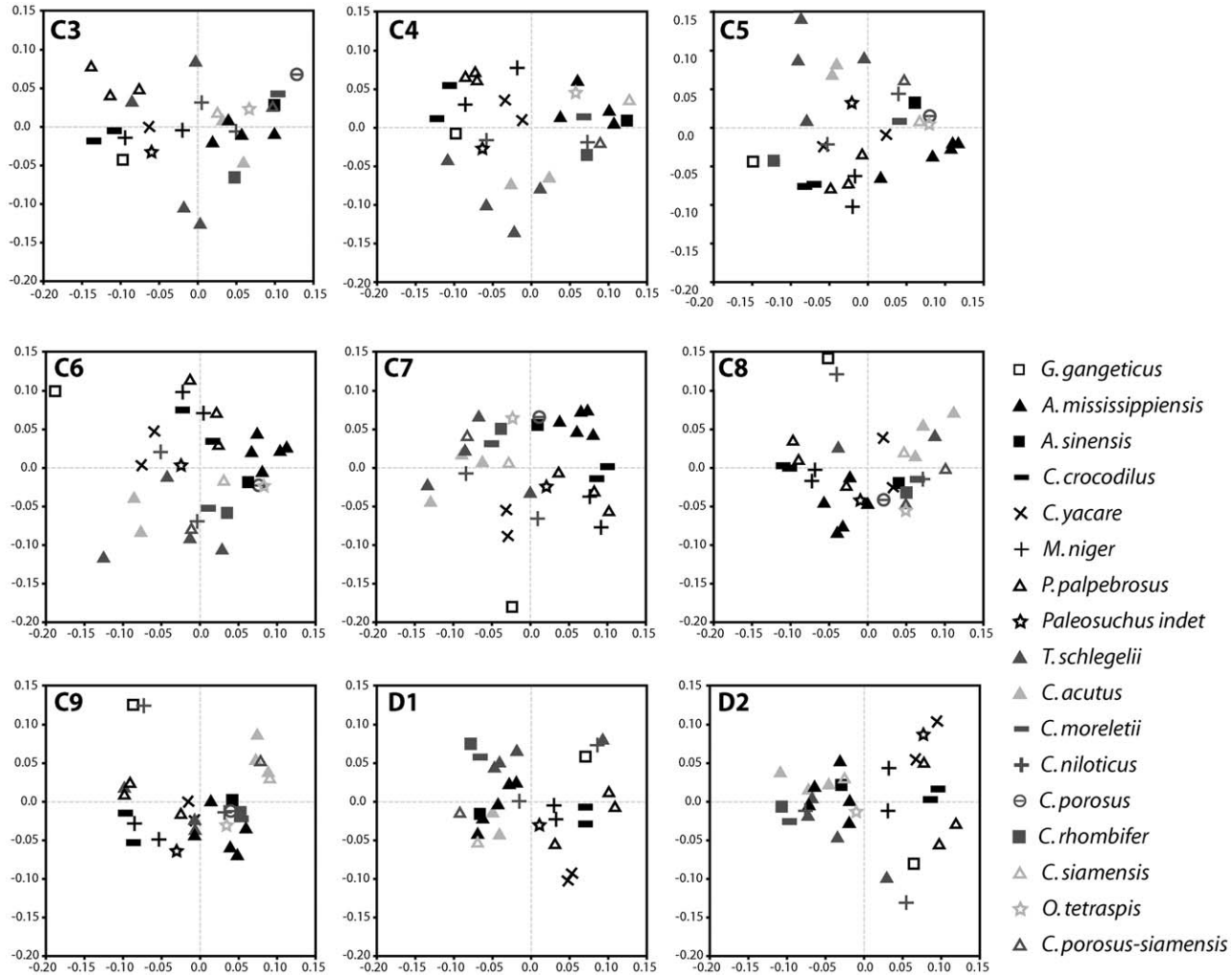

Fig. 5. PCA ordinations, and vertebral variation by position. Shape changes corresponding to the PCA axes are the same as those in Fig. 6.

Landmarks

Forty-three vertebral landmarks were digitized for 9 vertebrae in 32 specimens in three dimensions using a Microscribe G2 (Immersion, San Jose, CA). The landmarks (Fig. 2) capture the geometry of the vertebrae as conveyed by the shape of the articular surfaces, vertebral processes, and neural arch. Table 1 summarizes the anatomical terms used. Only the landmarks on the left half of each vertebra were analysed, with the exception of the prezygapophysis where it was necessary to include the landmarks on the right side to gain access to the morphology. The configurations of 3D landmarks were aligned using a full Procrustes fit to eliminate the effects of translation, rotation and scale, and centroid size. The most common measure of size in geometric morphometrics is centroid size (CS): the square root of the sum of all the squared distances between landmarks (Mitteroeker et al., 2013). Principal component analyses (PCA) were used to summarize the variance in shape data of each vertebral element across the sample (Lattin et al., 2003; Zelditch et al., 2004). The allometric relationship between vertebral shape and size was analysed using multivariate regression (Monteiro, 1999). All the geometric morphometric procedures were performed using MorphoJ (v.1.02c; Klingenberg, 2011). The visual morphs were obtained by exporting MorphoJ's results and warping a CT-scanned vertebra using Landmark Editor Software (Wiley, 2006).

In the present study we compare the results of the regional and the positional variations carried out in different analyses. First, we analysed the regional variation using PCA including crocodylids (Crocodylinae + *Tomistoma*), alligatorids and the gavial to determine the shape variation of the axial segment from C3 to D2. Second, we analysed the variation by element and position, which required an independent PCA (see sample number per vertebral position in Appendix 1) to envisage variation per positional site. These two analyses incorporate the taxonomic distinction between the two most diversified families. For regional variation the average vertebra of Crocodylidae and Alligatoridae were shaped using the pooled mean of the complete segment of the cervico-thoracic region. To assess the familiar differences we analyses each vertebral position separately using a discriminant analysis. A permutation test (1,000 permutations)

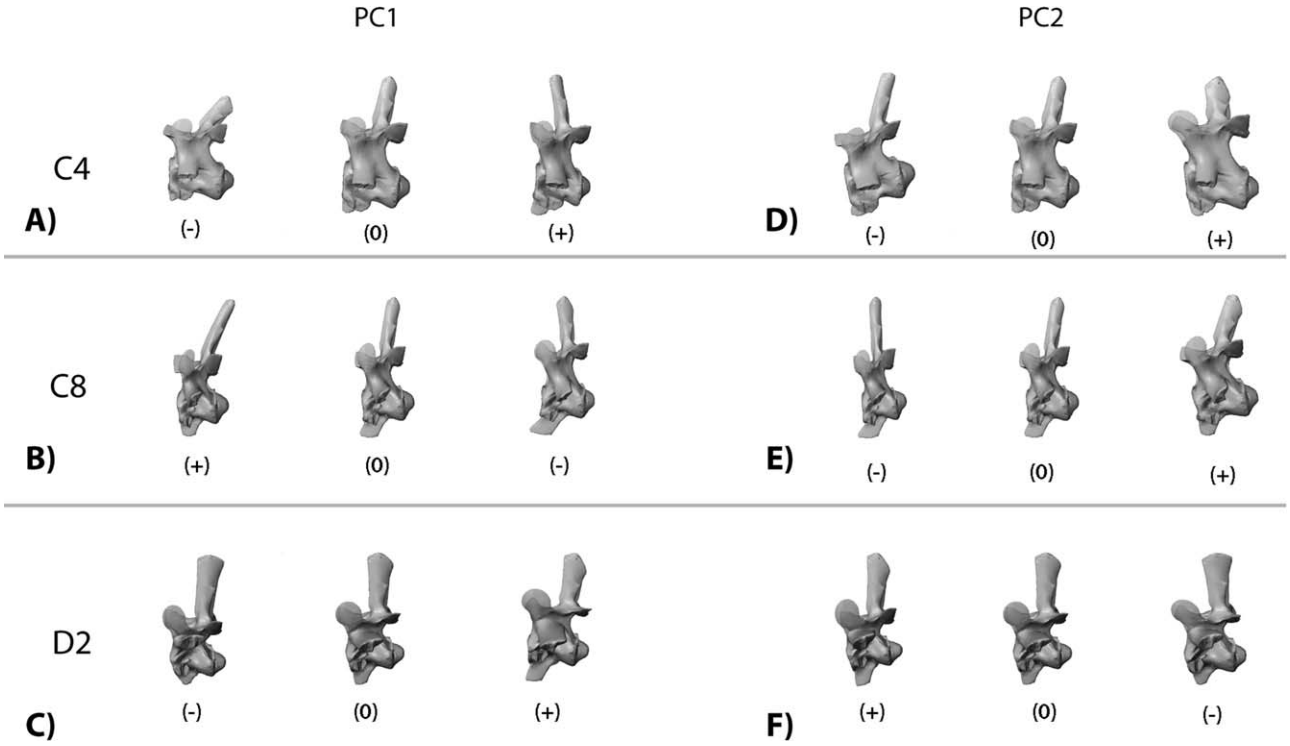

Fig. 6. Morphological variation across principal components by vertebral position. PC1 shown at left and PC2 at right; C4, C8, and D2 were used to exemplify shape variation. (**A**) Pattern of variation obtained in the analysis of C3, C4, C5, and C6 vertebrae; (**B**) the same at the interval C7 to C9; (**C**) the same for D1 and D2; (**D**) pattern of variation in PC2 obtained in the analysis of C3 to C6; (**E**) the same at the interval C7 to C9; (F) the same for D1 and D2.

using the Procrustes distance and the T^2 statistic were employed to identify any statistically significant difference in the mean shapes between the two families. Third, we evaluated the size of the intracolumnar variation to test the occurrence of regional differentiation. The ratio between the CS of each vertebra to the mean CS of each specific vertebral series has been calculated.

To test the effect of size on shape across the crocodylian species (interspecific allometry), a linear multivariant regression of the Procrustes residuals on size (CS) was performed to obtain the regression scores (RS, Drake and Klingenberg, 2008). We opted to use the raw (original) Procrustes data instead of using phylogenetically independent contrast because the data includes growth series, and the Crocodylinae interrelationships remain poorly resolved (*Crocodylus* species may even be fully polytomic). Moreover, *Tomistoma* may be the sister group of *Gavialis* or of Crocodylinae. All this would make the estimation of the hypothetical ancestors (HTUs) inconsistent with reality.

RESULTS

Regional Variation of the Cervico-thoracic Region

The same pattern of regional variation (i.e., intracolumnar) occurred irrespective of the taxon analysed, confirming that the axial patterning variation is conservative through all the species analysed (Fig. 3A). Most of the variation is explained by the first two principal components (PC1 = 51.16% and PC2 = 14.17%; variance explained = 65.33%; Table 2). The variation in shape explained by PC1 is principally related to changes in the orientation and the relative size of the para- and diapophyses (Fig. 3B). The changes in PC2 are associated with the cranio-caudal shorten of the centra, and the increase in height (relative to the neural arch and the vertebral body) of both the neural spines and the hypapophyses (Fig. 3C). In addition, the neural spine tends to be cranio-caudally shorter, with its axis perpendicular to the frontal plane of the vertebra.

In the scatter-plot (Fig. 3A) the vertebrae are ordered sequentially with respect to their anatomical position. There is a morphological gradation from the anterior to the posterior region (between C3 and D2), and the ordering of vertebrae is primarily determined by the variation in the dia- and parapophyses, which in turn determines the position of the vertebrae. Nevertheless, the morphological gradation showed a curved trajectory, which delimited two subset shape changes: the anterior series from C3 to C6, and the posterior from C7 to D2. Thus, the intracolumnar variation indicates a perceptible regionalisation of the axial patterning. Accordingly, between C3 and C6 the vertebrae are morphologically homogeneous. From C7 to D2 the vertebrae have a greater disparity in shape as a result of changes exerted by the para- and diapophyses (PC1). In these vertebrae (see negative values of PC1, Fig. 3B) the capitular facet of the parapophyses stretches cranio-caudally, and lengthens dorso-ventrally. Its position becomes more cranial and dorsal, situated near the neurocentral suture. The diapophyses tend to be oriented perpendicularly to the neural arch; lengthening their

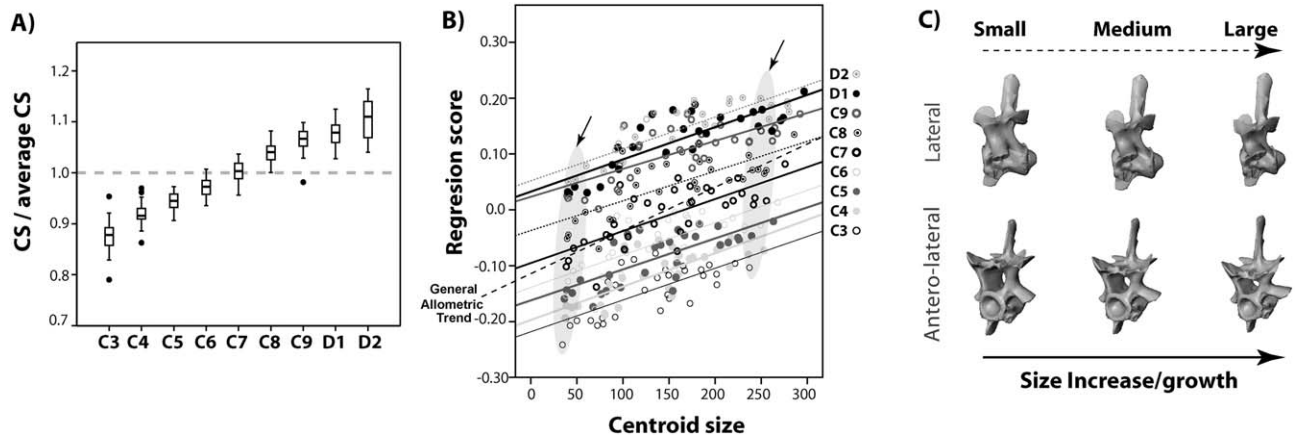

Fig. 7. Relationship between size and shape. (**A**) Box plot showing the standardized variation ordered from cranialmost (C3) to caudalmost (D2) vertebrae. The centroid size of each vertebra is standardized by the vertebrae mean size of the column they form part of. The line at CS = 1 denotes the mean size, above which the vertebrae are larger than the mean. (**B**) Multivariate regression analysis. The dispersion corresponds to the taxa ordered according to the correlation between size and shape (*x* size, *y* regression score, shape). Left arrow indicates the localization of both the younger *C. niloticus* and the smaller species *C. palpebrosus*, right arrow indicates an older and large individual of *C. niloticus*. The ellipse demarcates the total neck of each individual (from C3–D2). (**C**). Interspecific allometry per vertebral position predicted by the general allometric trend (dotted line in (B)).

positions change so that they are at the same level as the zygapophyses. In addition, in the two first thoracic vertebrate the neural spine widens cranio-caudally without changing orientation, and the hypapophyses are cranio-caudally shortened and ventrally oriented (see negative values of PC2, Fig. 3C).

Differences between crocodylids and alligatorids. A discriminant analysis of the families captures the morphological differences in the cervico-thoracic region ($P < 0.0001$; Fig. 4A). In this region, the average vertebra of crocodylids is characterized by their neural spine and arch. The neural arch is relatively short (cranio-caudally), and the spine is relatively long (dorso-ventrally) and pointed orthogonal to the frontal plane. Conversely, the average vertebra in alligatorids has a flattened and robust appearance, because the neural spine and the arch are cranio-caudally longer, with a relatively dorso-ventrally shorter spine. The hypapophysis is ventrally oriented and relatively smaller in crocodylids than in alligatorids (Fig. 4A). The facets of the zygapophyses are slightly bigger in crocodylids and the prezygapophysis occupies a more lateral position in the alligatorids.

Positional Variation

Particular local changes can be traced at the articular surfaces, neural arch and hypapohyses by examining the variation within each vertebral site. Most variation can be explained by the first two principal components (Fig. 5, Table 2). The variation across PC1 is characterized by the orientation of neural spine, the condyle, and the relative size and orientation of the hypapophysis (Fig. 6A–C). The results of PC1 for vertebrae C3 to C6 show scarcely any variation in the hypapophysis, the most noticeable change being at the condyle, and the neural spine orientation (Fig. 6A). The opposite occurs in the vertebrae C7 to D2 where there is more variation in the orientation and the relative size of the hypapophysis than in that of the condyle and the neural spine (Fig. 6B,C). The variation in the neural spine and hypapophysis is correlated, but opposed in the prothoracic (D1-D2) and cervical (C7-C9) vertebrae. In the two first thoracic vertebrae, the changes in caudally oriented neural spines are linked to large and cranially oriented hypapophyses, while orthogonally oriented neural spines are so with small and ventrally oriented hypapophyses (Fig. 6C). In PC2 (Fig. 6D–F) the variation involves the neural spine lamina, which is longer and thinner, or shorter and broader. Accordingly PC2, vertebrae (C7 to D2) with narrower spines have cranially oriented hypapophyses, while those with broader spines have vertically oriented hypapophyses (Fig. 6E,F).

Differences between crocodylids and alligatorids. At each vertebral position there are significant differences between alligatorids and crocodylids ($P < 0.0001$; Fig. 4B). Crocodylids necks are characterised by semispherical condyles facing dorsally, in particular throughout C3–C6, and by relatively long and narrow hypapophyses and neural spines throughout C5–C7. In crocodylids the diapophyses are more dorsally oriented than in alligatorids (Fig. 4B,C). The vertebral morphology of *Gavialis gangeticus* and *Tomistoma schlegelii* is similar to the pattern of variation observed in Crocodylinae. On the contrary, alligatorids have horizontally facing condyles (except in D2). The shape of C3–C4 and C6–D2 characterizes the cervico-thoracic series of alligatorids. The anterior vertebrae have broad neural spines caudally oriented but small hypapophysis (smaller than those of crocodylids), while the posterior vertebrae have large and cranially oriented hypapophysis (larger than those of crocodylids; Fig. 4B,C).

Size

Across taxa, the average centroid size of vertebrae increases orderly from the third cervical to the last second

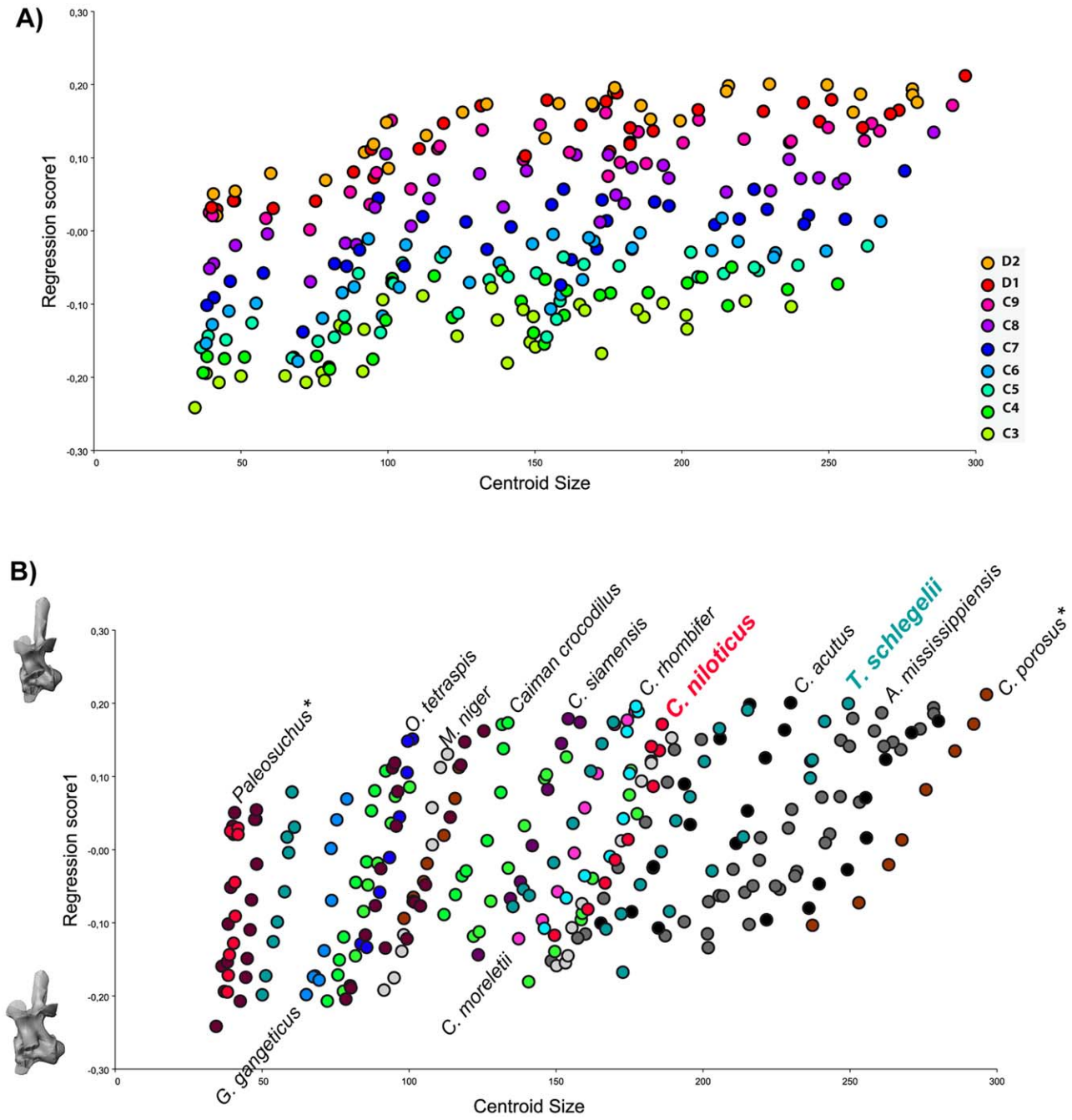

Fig. 8. Color-coded ordination of multivariate regression of Fig. 7 showing the relationship between vertebral size and shape. (**A**) Color coding indicates vertebral positions across species. (**B**) Color coding separates between species in the sample. Two growth series are highlighted coloring the species' names (*Tomistoma schlegelii* and *Crocodylus niloticus*) and asterisk highlights the size difference between the smallest and the largest species in the sample.

thoracic; the most rostral vertebrae (C3–C4) are the smallest and the most caudal vertebrae (D1–D2) the largest (isometry; Fig. 7A). When analysing the complete dataset (i.e., neither taking into consideration the position nor taxonomy), the multivariate regression yields an ordered pattern that allows differentiating both neck configurations (by vertebral position) and species (Fig. 8A,B). Accordingly, the multivariate regression of shape onto CS shows a general trend in which vertebral shape changes allometrically (%explained variance = 7.04; $P < 0.0001$; Fig. 7B), and whereby growth (size increase) predicts changes in the vertebral centrum and the neural spine (Fig. 7C). This covariance between size and shape across species corresponds to the interspecific allometry of the cervico-thoracic region. Interestingly, the allometric scaling (slope) of each vertebra,

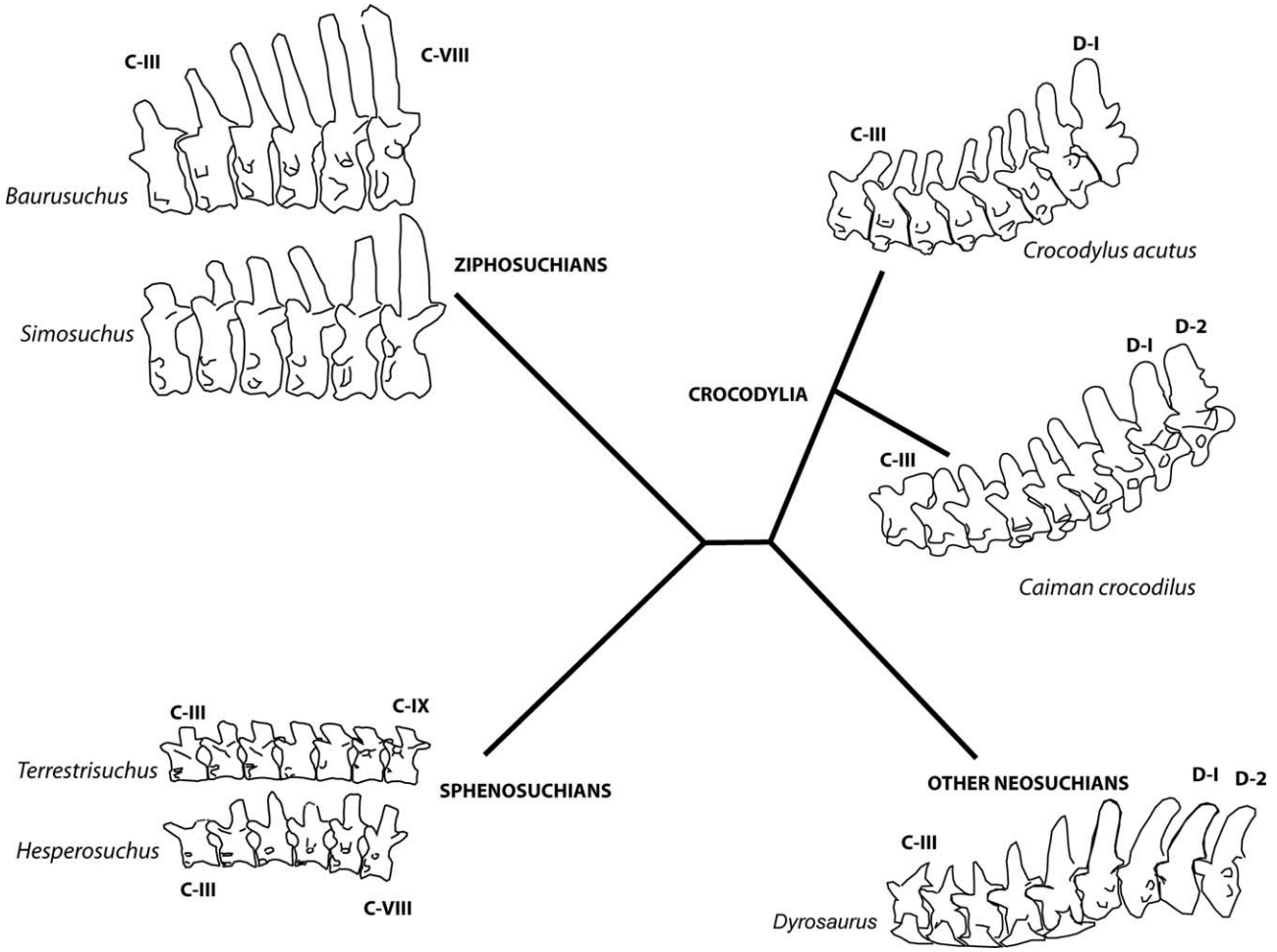

Fig. 9. Phylogenetic network of Crocodylomorpha, showing the axial neck patterning (not scaled) of *Terrestrisuchus gracilis* (Crush, 1984); *Hesperosuchus agilis* (Colbert, 1952), *Simosuchus clarki* (Georgi and Krause, 2010), *Baurusuchus albertoi* (Nascimento and Zaher, 2010) and *Dyrosaurus maghribensis* (Jouve et al., 2006) compared with *Crocodylus acutus* and *Caiman crocodilus*. Despite the diversity of Neosuchia, there are few complete specimens with well-preserved articulated necks. Abbreviations: C, cervical; D, dorsal.

compared by position, is equivalent to that of the general trend (i.e., size increase explains equivalent shape changes), although the trends are parallel, clearly indicating that they differ in the intercept. Furthermore, a posterior analysis (PCA) of the residuals (the portion of shape variance which is not correlated to size), indicates that the total range of shape variance, which was previously explained in Fig. 3A,B, is non-allometric (i.e., differences in the intercept indicate that major shape changes across crocodylians are size independent). Consequently, this not only indicates that the major source of variation in cervico-thoracic region is independent of size, but also that the observed allometric patterns (whether the general or the positional trends) derives from the fact that in the sample there are younger and older individuals (e.g., *Crocodylus niloticus*), plus the smaller and larger species (e.g., *Caiman palpebrosus* and *Crocodylus porosus-siamensis*, respectively). This further suggests that both the ontogenetic and interspecific allometric trends explain the same vertebral shape changes.

DISCUSSION

Vertebral series contain important morphological information, from embryology to local changes of its parts, which relate to the evolution of axial column patterning (Filler, 1986, 2007). When combined, both the analyses of regional variation and those of variation by element and position (i.e., intracolumnar and interspecific patterns of neck morphological variation, respectively) indicate that patterns of intracolumnar variation encompass gradual shape changes in the vertebral series, and that the cervico-thoracic region is quite conservative among extant crocodylians. However, we also found that there are statistically significant taxonomic differences in vertebral position in the necks between crocodylian families. These differences are mainly encompassed by the neural spine, the neural arch and the hypapophysis, and together, these convey a significant average neck vertebra between families.

Our results substantiate that the positions of para- and diapophyses and other vertebral processes, such as

the pre- and postzygapohyses, are responsible for much of the variation in crocodilian necks (Mook, 1921). However, we found that these differences are independent of body size. Arguably, this may be related to the fact that the cervical and prothoracic shape differentiation takes place during early crocodylian ontogeny (Brochu, 1996; Salisbury and Frey, 2001; Ikejiri, 2012), entailing that the shape of structures such as the para- and diapophyses, the condyle, and the neural spine would take place during post hatching stages. This latter observation is in agreement with the results of the multivariate regression. A statistically significant trend was found which indicated that size differences among vertebrae of equivalent position, across the sample, imply subtle and equivalent allometric differences. Moreover, all the neck vertebrae appear to be equally scaled through their ontogeny and interspecifically. The result of this equivalence in intracolumnar shape differentiation and scaling is what conveys the appearance of a conservative axial patterning to crocodylians, and is congruent with the conservativeness of the neck muscular arrangement across species (Tsuihiji, 2005, 2007).

Notwithstanding the above, the level of intracolumnar shape differentiation is sufficient to allow distinguishing between two sub regions (i.e., C3–6 and C7–D2, see also PC1 and PC2; Fig. 3). Interestingly, the vertebrae along the C3–C6 subregion are smaller than the rest, and comprise a serially organized segment in which cervical ribs are highly imbricated. This segment corresponds to a portion of the neck which has restricted mobility (Salisbury and Frey, 2001). There is also a striking match between the morphological distinctness between the sub regions (those allocated by the analysis), and two different domains of *Hox* expression in the early embryo. Specifically, recent studies in molecular genetics have shown that in *Alligator mississippiensis* the separation between regions C3–C6 and C5–D1 are determined by the *Hoxb*−4 and *Hoxc*−4 complexes, respectively (Mansfield and Abzhanov, 2010). Examples of these types of morphological and molecular genetic matches have been documented in mammals, but in the absence of a mechanistic rationale, their assessment has, so far, only been tentative (Kessel and Gruss, 1991).

Our results clearly demonstrate that there are differences in the neck vertebrae of Crocodylia that could prove to be a useful tool in the identification, classification and evolution of this interesting group of animals. There are taxonomic differences in the neck configurations of Alligatoridae and Crocodylidae (Fig. 4). However, to date, most of the vertebral characters described in the literature, and which have been used for phylogenetic inference, are based on proatlas and axis morphology (Fig. 1). Geometric morphometrics enabled us to discern both serial and local characters for taxonomy (Figs. 5 and 6), although their application on phylogenetic inference must be taken thoughtfully (i.e., phylogenetically characters are discrete units while in morphometrics are continuous). For instance, according to our analyses, the grouping of Caimanines (*Paleosuchus*, *Melanosuchus*, and *Caiman*) is characterized by a lower and craniocaudally wider C3 neural spine, and by the craniocaudal expansion of neural spines and zygapophyses at the prothoracic vertebrae. In addition, the vertebrae C6 and C7 accurately separate Alligatoridae and Crocodylidae. These vertebrae have shorter neural spines and cranially directed hypapophyses in alligatorids, but tall and narrow neural spines and orthogonal hypapophyses in crocodylids (including *Osteolaemus* and *Tomistoma)*. The separation of the specimens in the sample into two families indicates that the combination of all these features is not related to any particular maturation stage for C6 and C7 vertebrae. It is noteworthy that the single *Gavialis* specimen tends to group with the crocodylids.

Postnatal growth may be the principal cause for neck divergence between crocodylian families if one considers an average alligatorid neck vertebra (with wider craniocaudal neural spines and arches, and lower spines than crocodylids), because neurocentral fusion during growth in *Alligator mississippiensis* is delayed when compared with the rest of crocodilians (Ikejiri, 2012). In effect, an allometric consequence of the delay in neurocentral fusion in the *Alligator* is the acquisition of wider neural spines and longer centra at the anterior-most cervical vertebrae (Ikejiri, 2010). This agrees with the pattern of variation that we observed for the cervical elements in all of the alligatorids, enabling to hypothesize that the timing of neurocentral fusion in the latter group may explain the differences in the configuration of the Alligatoridae neck.

Differences in the necks of Crocodylomorpha at a macroevolutionary scale have not been yet traced. However, the few examples of complete neck organization in extinct groups suggest that the intracolumnar patterns of the neck support the clusters of clades. Compare, for instance, the axial neck patterning of sphenosuchians with that of ziphosuchians (Fig. 9). Sphenosuchians show low neural arches and spines of sub-equal width and rather long centra, while ziphosuchians have high neural arch pedicels, an increasing length of neural spines and short centra. In turn, Alligatoridae and Crocodylidae share a particular neck organization when compared with other crocodylomorph groups (Fig. 9), possibly entailing a key evolutionary innovation. The intracolumnar serial pattern that we addressed above entails morphological differences at particular vertebral position, which split the neck in two distinct subregions. A similar organization also occurs in the specialized axial column of *Dyrosaurus* (Jouve et al., 2006), which denotes a common phylogenetic axial patterning at the level of Neosuchia, if not a convergence.

CONCLUSIONS

One of the main advantages of geometric morphometrics is the ability of this technique to segregate isometric size from the landmark configurations, enabling the assessment of patterns of shape variation and allometry in a unique way. Relying on this advantage, we have been able to demonstrate that vertebral shape variation can be abstracted with a set of landmarks extensible to other related archosaurs. On these bases, we have found that the general shape variation of a complex and serially ordered structure such as the crocodylian neck is nearly identical across taxa. Moreover, only a small portion of this shape variation is coupled with size (allometry), yet surprisingly, the neck vertebrae in crocodylians share the same ontogenetic and interspecific allometric trends. This phenomenon likely conveys the paradigmatic conservativeness of the morphological organization

of the neck in crocodylians. In spite of this, there are local (positional) nuances that make each family's neck subtly characteristic. Arguably, the fact that most of the neck's morphological variation is independent of size (allometric trends differ in the intercept), suggests that vertebral differences possibly arise early in ontogeny. These results open a prospect to further study the evolutionary transformation in Crocodylomorpha, including their fossil record.

ACKNOWLEDGEMENTS

The authors thank Dr. Kenneth L. Krysko and Dr. Max A. Nickerson (Florida Museum of Natural History, Gainesville, Florida) and Museo del Cocodrilo (Instituto de Historia Natural y Ecología, Estado de Chiapas, México) for access to the specimens in their care. They are also grateful to Dr. Santiago Reig Redondo who dramatically perished in an accident, and to his team (Laboratorio de Imagen Médica, Hospital General Universitario Gregorio Marañón, Madrid) for CT-scanning the vertebrae used as a template in most of the figures. Patricia Taylor has improved the English language of our original manuscript. Daniela Schwarz and an anonymous referee gave helpful comments on the manuscript.

LITERATURE CITED

Benton MJ, Clark JM. 1988. Archosaur phylogeny and the relationships of the Crocodylia. In: Benton MJ, editor. The phylogeny and classification of the tetrapods. Vol. 1: Amphibians, reptiles, birds. Oxford: Clarendon Press (The Systematics Association Special Volume 35A). p 295–338.

Brochu CA. 1992. Late-stage ontogenetic changes in the postcranium of Crocodylians. J Vertebr Paleontol 12:19A.

Brochu CA. 1996. Closure of neurocentral sutures during crocodilian ontogeny: implications for maturity assessment in fossil archosaurs. J Vert Paleontol 16:49–62.

Brochu CA. 1997. Morphology, fossils, divergence timing, and the phylogenetic relationships of *Gavialis*. Syst Biol 46:479–522.

Burnell A, Collins S, Young BA. 2012. Vertebral morphometrics in *Varanus*. Bull Soc Géol France 183:151–158.

Busbey AB. 1994. Structural consequences of skull flattening. In: Thomason JJ, editor. Functional morphology in vertebrate paleontology. Cambridge: University Press. p 173–192.

Buscalioni AD, Piras P, Vullo R, Signore M, Barbera C. 2011. Early eusuchia crocodylomorpha from the vertebrate-rich Plattenkalk of Pietraroia (Lower Albian, southern Apennines, Italy). Zool J Linnean Soc 163:S199–S227.

Chen X, Milne N, O'Higgins P. 2005. Morphological variation of the thoracolumbar vertebrae on macropodidae and its functional relevance. J Morphol 266:167–181.

Claessens L. 2009. A cineradiographic study of lung ventilation in *Alligator mississippiensis*. J Exp Zool 311A:563–585.

Cleuren J, De Vree F. 2000. Feeding in crocodilians. In: Schwenk K, editor. Feeding: form, function, and evolution in tetrapod vertebrates. San Diego: Academic Press. p 337–358.

Colbert EH. 1952. A pseudosuchian reptile from Arizona. B Am Mus Nat Hist 99:565–592.

Cong LY, Hou LH, Wu XC, Hou JF. 1998. The gross anatomy of *Alligator sinensis* Fauvel. Beijing: Academia Sinica.

Crush PJ. 1984. A late Upper Triassic sphenosuchid crocodilian from Wales. Palaeontology 271:131–157.

Drake AG, Klingenberg CP. 2008. The pace of morphological change: historical transformation of skull shape in St Bernard dogs. Proc R Soc B 275:71–76.

Duncker HR. 1979. Coelomic cavities. In: King AS, McLelland J, editors. Form and function in birds. Vol. 1. New York: Academic Press. p 39–67.

Filler AG. 1986. Axial character seriation in mammals: an historical and morphological exploration of the origin, development, use and current collapse of the homology paradigm. PhD Thesis. Cambridge: Harvard University.

Filler AG. 2007. Homeotic evolution in the mammalia: diversification of therian axial seriation and the morphogenetic basis of human origins. PLoS One 2:1–23.

Frey E. 1988a. Das Tragsystem der Krododile—eine biomechanische und phylogenetische Analyse. Stutt Beitr Naturk Series A 426:1–60.

Frey E. 1988b. Anatomie des Körperstammes von *Alligator mississippiensis* Daudin. Stutt Beitr. Naturk Series A 424:1–106.

Galliari FC, Carlini AC, Sánchez-Villagra MR. 2009. Evolution of the axial skeleton in armadillos (Mammalia, Dasypodidae). Mamm Biol 75:326–333.

Georgi JA, Krause DW. 2010. Postcranial axial skeleton of *Simosuchus clarki* (Crocodyliformes: Notosuchia) from the Late Cretaceous of Madagascar. J Vertebr Paleontol 30:99–121.

Hoffstetter R, Gasc JP. 1969. Vertebrae and ribs of modern reptiles. In: Gans C, Bellairs A, Parsons TS, editors. Biology of the reptilia. Vol. 1. London: Academic Press. p 201–310.

Ikejiri T. 2010. Morphology of the neurocentral junction during postnatal growth of *Alligator* (Reptilia, Crocodylia). PhD Thesis. University of Michigan.

Ikejiri T. 2012. Histology-based morphology of the neurocentral synchondrosis in *Alligator mississippiensis* (Archosauria, Crocodylia). Anat Rec 295:18–31.

Johnson RG. 1955. The adaptive and phylogenetic significance of vertebral form in snakes. Evolution 9:367–388.

Jouve S, Iarochène M, Bouya B, Amaghzaz M. 2006. A new species of *Dyrosaurus* (Crocodylomorpha, Dyrosauridae) from the early Eocene of Morocco: phylogenetic implications. Zool J Linnean Soc 148:603–656.

Kessel M, Gruss P. 1991. Homeotic transformations of murine vertebrae and concomitant alteration of *Hox* codes induced by retinoic acid. Cell 67:89–104.

Klingenberg CP. 2011. MorphoJ: an integrated software package for geometric morphometrics. Mol Ecol Resour 11:353–357.

Lattin J, Carrol JD, Green PE. 2003. Analyzing multivariate data. Canada: Thomson Learning, Inc.

Manfreda M, Mitteroecker P, Bookstein FL, Schaefer K. 2006. Functional morphology of the first cervical vertebra in humans and nonhuman Primates. Anat Rec 289B:184–194.

Mansfield JH, Abzhanov A. 2010. Hox expression in the American *Alligator* and evolution of archosaurian axial patterning. J Exp Zool 314B:1–16.

Mitteroecker P, Gunzb P, Windhagerc S, Schaefer K. 2013. A brief review of shape, form, and allometry in geometric morphometrics, with applications to human facial morphology. Hystrix 24: 59–66.

Monteiro LR. 1999. Multivariate regression models and geometric morphometrics: the search for causal factors in the analysis of shape. Syst Biol 48:192–199.

Mook CC. 1921. Notes on the postcranial skeleton in the Crocodilia. B Am Mus Nat His 44:67–100.

Mook CC. 1925. A revision of the Mesozoic crocodilia of North America. B Am Mus Nat His 51:319–432.

Nascimento PM, Zaher H. 2010. A new species of *Baurusuchus* (Crocodyliformes, Mesoeucrocodylia) from the Upper Cretaceous of Brazil, with the first complete postcranial skeleton described for the family Baurusuchidae. Pap Avulsos Zool 50:323–361.

Norell MA. 1989. The higher level relationships of the extant Crocodylia. J Herpetol 23:325–335.

Pol D, Turner AH, Norell MA. 2009. Description of a new specimen of the Late Cretaceous crocodylomorph *Shamosuchus djadochtaensis* and a discussion of neosuchian phylogeny as related to the origin of Eusuchia. B Am Mus Nat Hist 324:1–103.

Polly PD, Head JJ. 2004. Maximum-likelihood identification of fossils: taxonomic identification of Quaternary marmots (Rodentia, Mammalia) and identification of vertebral position in the

pipesnake *Cylindrophis* (Serpentes, Reptilia). In: Elewa AMT, editor. Morphometrics: applications in biology and paleontology. Heidelberg: Springer Verlag. p 117–221.
Rieppel O. 1993. Studies on skeleton formation in reptiles. V. Patterns of ossification in the skeleton of *Alligator mississippiensis* DAUDIN (Reptilia, Crocodylia). Zool J Linnean Soc 109:301–325.
Romer AS. 1956. The osteology of the reptiles. Chicago: The University of Chicago Press.
Salisbury SW, Frey E. 2001. A biomechanical transformation model for the evolution of semi-spheroidal articulations between adjoining vertebral bodies in crocodilians. In: Grigg GC, Seebacher F, Franklin CE, editors. Crocodilian biology and evolution. Australia: Surrey Beatty & Sons. p 85–134.
Salisbury SW, Molnar RE, Frey E, Willis PMA. 2006. The origin of modern crocodyliforms: new evidence from the Cretaceous of Australia. Proc Roy Soc Lond B Bio 273:2439–2448.
Sarris I, Marugán-Lobón J, Chamero B, Buscalioni AD. 2012. Shape variation and allometry in the precloacal vertebral series of the snake *Daboia russelli* (Viperidae). Int J Morphol 30:1363–1368.
Schachner ER, Lyson TR, Dodson P. 2009. Evolution of the respiratory system in nonavian theropods: evidence from rib and vertebral morphology. Anat Rec 292:1501–1513.
Schwarz D, Frey E, Martin T. 2006. The postcranial skeleton of the Hyposaurinae (Dyrosauridae; Crocodyliformes). Palaeontology 49: 695–718.
Seidel MR. 1978. The somatic musculature of the cervical and occipital regions of *Alligator mississippiensis*. Unpublished PhD Thesis. New York: The City University of New York.
Troxell EL. 1925. *Thoracosaurus*, a Cretaceous crocodile. Am J Sci 5:219–233.
Tsuihiji T. 2005. Homologies of the *transversospinalis* muscles in the anterior presacral region of sauria (crown Diapsida). J Morph 263:151–178.
Tsuihiji T. 2007. Homologies of the *longissimus, iliocostalis* and hypaxial muscles in the anterior presacral region of extant Diapsida. J Morph 268:986–1020.
Wake MH. 1980. Morphometrics of the skeleton of *Demorphis mexicanus* (Amphibia: Gymnophiona). Part I. The vertebrae, with comparisons to other species. J Morphol 165:117–130.
Wiley DF. 2006. Landmark Editor 3.0. Institute for data analysis and visualization, University of California. Available at: http://graphics.idav.ucdavis.edu/research/EvoMorph.
Zelditch ML, Swiderski D, Sheets D, Fink W. 2004. Geometric morphometrics for biologist: a primer. London: Elsevier.

APPENDIX

List of specimens and vertebrae sampled

Species	Individual	C3	C4	C5	C6	C7	C8	C9	D1	D2	Fem. Length
A. mississippiensis	UF 39106	X	X	X	X	X	X	X	X	X	180
A. mississippiensis	UF 33552	X	X	X	X	X	X	X	X	X	235
A. mississippiensis	UF 42548	X	X	X	X	X	X	X	X	X	–
A. mississippiensis	UF 35129	X	X	X	X	X	X	X	X	X	243
A. mississippiensis	UF 39618	X	X	X	X	X	X	X	X	X	256
A. sinensis	UF105540	X	X	X	X	X	X	X	X	X	134
C. crocodilus	UF45438	X	X	X	X	X	X	X	X	X	87
C. crocodilus	UF45439	X	X	X	X	X	X	X	X	X	97
C. yacare	UF120653	0	X	X	X	X	X	X	X	X	131
C. yacare	UF121232	X	X	X	X	X	X	X	X	X	160
M. niger	UF66428	X	X	X	X	X	X	X	X	X	110
M. niger	UF72914	X	X	X	X	X	X	X	X	X	167
P. palpebrosus	UF72815	X	X	X	X	X	X	X	X	0	44
P. palpebrosus	UF75020	X	X	X	X	X	X	X	X	X	–
P. palpebrosus	UF75023	X	X	X	X	X	X	X	X	X	88
Paleosuchus	UAM	X	X	X	X	X	X	X	X	X	–
C. acutus	UF54201	X	0	0	0	X	X	X	X	X	205
C. acutus	UF56580	X	X	X	X	X	X	X	X	X	246
C. acutus	UF98068	X	X	X	X	X	X	X	X	0	195
C. moreleti	UF54813	X	X	X	X	X	X	X	X	X	165
C. niloticus	UF115639	X	X	X	X	X	X	X	X	X	46
C. niloticus	UF54812	X	X	X	X	X	X	X	X	X	178
C. porosus	UF63931	X	X	X	X	X	X	X	0	0	–
C. porosus-siamensis	UF69364	X	X	X	X	X	X	X	X	0	262
C. rhombifer	UF45189	X	X	X	X	X	X	X	X	X	185
C. siamensis	UF71182	X	0	X	X	X	X	X	X	X	149
O. tetraspis	UF33749	X	X	X	X	X	X	X	X	X	98
T. schlegelii	UF72817	X	X	X	X	X	X	X	X	X	59
T. schlegelii	UF54210	X	X	X	X	X	X	0	X	X	151
T. schlegelii	UF107493	X	X	X	X	X	X	X	X	X	203
T. schlegelii	UF84888	X	X	X	X	X	X	X	X	X	193
G. gangeticus	UF70592	X	X	X	X	X	X	X	X	X	78
		31	30	31	31	32	32	31	31	28	Total = 277

For each specimen, the absence of particular vertebrae is specified as (0). The last row corresponds to the number of vertebrae used in the multivariate analysis by vertebral position. *Fem. Length* lists the linear length of the femur (in mm) denoting the degree of maturity. Institutional Abbreviations: UF, Florida Museum of Natural History; UAM, Universidad Autónoma Madrid.